JAAS

Dynamic Article Links

Cite this: *J. Anal. At. Spectrom.*, 2011, **26**, 2281

www.rsc.org/jaas

PAPER

Effect of particle size distribution in laser-induced breakdown spectroscopy analysis of mesoporous V–SiO_2 catalysts

Miloslav Pouzar,*[a] Tomáš Kratochvíl,[a] Saara Kaski,[b] Jozef Kaiser,[c] Petr Knotek,†[d] Libor Čapek[e] and Tomáš Černohorský[a]

Received 1st June 2011, Accepted 23rd August 2011
DOI: 10.1039/c1ja10167f

In this paper, the effect of particle size on Laser-Induced Breakdown Spectroscopy (LIBS) analysis of mesoporous V–SiO_2 catalyst samples was investigated. The measurements were realized on three LIBS devices with different parameters. Concentrations of V in samples used for LIBS experiments previously determined by inductively coupled plasma-optical emission spectroscopy (ICP-OES) varied from 1.2 to 4.7 w/w%. Granulometry of silica samples was modified by two grinding methods (conventional vibration mill and cryogenic mill) and three sets of samples with different particle size distributions were obtained. Ground samples were then deposited in the form of a thin layer on the adhesive tape and analysed by LIBS. Curves describing the relationship between the vanadium concentration and the corresponding intensity of LIBS signal (*C–I* curves) were constructed for all three groups of samples, with different granulometry profiles measured with three different LIBS devices. The *C–I* curves for samples with narrow particle size distribution showed the highest values of slopes. Detection limits achieved were in the range 0.063–0.012% (w/w). The best LOD values were obtained for samples with the lowest mean particle size.

Introduction

Laser-Induced Breakdown Spectroscopy (LIBS) is an analytical technique based on the evaluation of the optical emission spectra of the plasma produced by the interaction of a high-power laser with the sample. Typical optical intensities on the sample surface can reach MW mm^{-2}. This technique provides multielemental, quasi non-destructive analysis that is useful, *e.g.*, for fast measurement of a little amount (down to ng) of analyte, with minimal sample preparation.[1–3] Even if the laser-induced plasma (LIP) characteristics are mainly dependent on the laser parameters, the physical and chemical properties of the sample (absorptivity, grain size, surface roughness, and thermal conductivity) can largely influence the generated plasma conditions. This phenomenon, well known also for another laser-ablation based analytical technique, *e.g.*, for laser ablation inductively coupled plasma mass spectrometry (LA-ICP-MS),[4,5] is the matrix effect. The intensity of the observed LIBS emission lines is directly proportional to the concentration of atoms in an appropriate energetic state in LIP. An important factor that influences the concentration of atoms in plasma is the matrix effect. The accuracy of qualitative and quantitative LIBS analysis is strongly affected by the mentioned matrix effect; therefore, it is very important to understand this phenomenon for the future developments of this technique.[6–11]

The problem of matrix effects in LIBS has been addressed in numerous publications. Earlier works concerned mainly the methods of matrix effect correction.[6–11] Systematically, the matrix effect for selected LIBS applications was studied by Borisov *et al.*[12] and Margetic *et al.*[13] They investigated the effect of the laser pulse length on the LIBS analysis of Cu–Zn alloys and stated that the emission intensities of the spectral lines depend non-linearly on the laser pulse duration (pico- and femto-second). This effect correlated with the changes in the mass ablation rate.

Bulatov *et al.*[14] and Krasniker *et al.*[15] found that the matrix effect is influenced by the amount of energy coupled to the plasma. This amount can be related to the velocity of the shock waves involved during plasma formation and growth. According to the authors, the matrix effect was linked to the ionization potential of elements in the sample. Easily ionized elements provided higher emission in contrast with hardly ionized elements, which contributed mainly to the first stages of plasma formation.

[a]*University of Pardubice, Institute of Environmental and Chemical Engineering, Studentska 573, 532 10 Pardubice, Czech Republic*
[b]*University of Jyväskylä, Department of Chemistry, P.O. BOX 35, 40014 University Jyväskylä, Finland*
[c]*Brno University of Technology, Institute of Physical Engineering, Technická 2896/2, 616 69 Brno, Czech Republic*
[d]*University of Pardubice, Faculty of Chemical Technology, Studentska 573, 532 10 Pardubice, Czech Republic*
[e]*University of Pardubice, Department of Physical Chemistry, Studentska 573, 532 10 Pardubice, Czech Republic*
† Present address: Joint Laboratory of Solid State Chemistry of Institute of Macromolecular Chemistry Academy of Sciences of Czech Republic, v.v.i., and University of Pardubice, Studentska 84, 532 10 Pardubice, Czech Republic.

Kningt *et al.*[16] used LIBS for stand-off elemental analysis of geological and other samples in a simulated Mars atmosphere (7 Torr, CO_2 atmosphere, distance 19 m). The calibration curves were prepared using a set of synthetic silicate standards with a uniform bulk matrix composition, but having significant variations in trace and minor elements and from measurements of stream sediment samples with variations in the concentration of major elements composing the matrix. The calibration curves for Sr showed good linearity in the case of samples having the same bulk compositions, while different bulk compositions calibration curves were significantly less linear. Similar results, showing greater difference between the two curves, were obtained for other elements. The physical states of the used samples were identical and all were ground to powders of uniform size.

Eppler *et al.*[17] investigated the effect of chemical speciation and matrix composition on Pb and Ba analysis in soil and sand. The relationship between ratios of the signal from matrix elements to the signal from trace elements of the analyte was studied. They found that the emission intensities are affected by the physical properties of the compound (enthalpy of formation, enthalpy of vaporization, Gibbs free energy, entropy, enthalpy of fusion, heat capacity and molar volume). The chemical compound and bulk sample composition (different proportions of soil and sand in a soil/sand mixture) were also influencing the emission signal. Similarly to Bulatov *et al.*[14] and Krasniker *et al.*,[15] they concluded that the matrix effect is caused by different ionization potentials of the elements in the sample. They also stated that matrix absorptivity influences the emission signal.

In the work of Ismail *et al.*[18], the matrix effect on the LIBS LODs for four elements (Mg, Si, Mn, and Cu) in two different matrices (aluminium and steel standard alloys) was studied. Mn and Cu calibration curves showed good linearity in steel samples, while Mg had the best calibration curve in the case of aluminium samples. This phenomenon was attributed to the physical properties of the investigated trace and matrix elements. Mn and Cu have certain physical properties (atomic weight, boiling point, melting point, specific heat, density, and ionization potential) closer to Fe and far from Al properties. This can result in a change of emission intensities due to the energy convection between the elements within the matrix. The similar behaviour was observed in the case of Mg and Si measurement.

Gornushkin *et al.*[19] investigated the influence of the matrix on the Mg detection by LIBS using a wide range of NIST certified reference materials with different bulk compositions. Powdered samples in the form of thin layers on adhesive tape were utilized, with a close-to monolayer distribution of the powder on the tape. With correction for the sample surface density on the tape (that was determined by weighing before and after sample deposition), a reasonable relative error and a precision were obtained for the determination of Mg in several certified samples. A calibration plot was constructed from homogeneous graphite samples doped with Mg. The authors concluded that the mass of the sample ablated into the LIP is the most important parameter in the analysis of powdered samples. The different grain sizes and densities of the samples can cause different masses released by the laser beam.

Anzano *et al.*[20] compared the matrix effects for powdered samples in the form of pressed pellets and samples deposited on adhesive tape. They used synthetic model samples prepared from various iron and aluminium compounds spiked with SiO_2 and $CaCO_3$ matrices. The samples were ground and mixed to ensure the homogeneity of the particles. Part of the obtained powder was pressed into pellets and the other part stuck using a double-sided tape on a slide. Matrix effects were investigated by monitoring the changes in calibration curve slopes after adding SiO_2 or $CaCO_3$ to the samples. The effect of the adding matrices was observed only in the case of tablets. In the case of Fe in $CaCO_3$, the slope of the calibration line decreased by more than 40%. The same effect was observed in samples with Al. A significant effect of particle diameters on the emission intensity and accuracy was observed. Particles with diameters larger than about 100 μm provided results with an error less than 2%. The authors assumed that this phenomenon can be explained by the different amounts of ablated material. In the case of smaller particles (powder samples), a smaller amount of material was ablated and the lower emission intensity was recorded. According to the authors, the powder deposited on the tape materials behaves similarly in terms of physical properties and, therefore, the matrix effect is insignificant. The matrix effects were attributed mainly to differences in the distribution of particle sizes.

In our work, the matrix effect on the quantitative LIBS analysis of vanadium in hexagonal mesoporous silica catalysts was studied. A detailed investigation of the influence of the particle size and particle size distribution on the LIBS signal is presented. The three LIBS setups in analysis of silica catalysts were systematically compared. As a sample preparation method, deposition of the powdered samples on the surface of adhesive tape was adopted.

Experimental

Sample preparation and characterization

The objective of this work is to study the effect of the sample's particle size diameter and distribution on the reproducibility and sensitivity of the LIBS analysis. For these purposes, an analyte with a clearly defined matrix (from a chemical point of view) was needed, with the ability to create samples with different particle size distributions and appropriate concentration ranges of the measured element. Therefore, samples of mesoporous V–SiO_2 catalysts were chosen and their subsequent treatment was performed by different grinding techniques (see Table 1).

The concentration of vanadium in untreated samples was measured by ICP-OES. Samples were analyzed after microwave digestion in solution of HF, HNO_3, HCl and H_3BO_3. The measurement was carried out with the sequential, radially viewed ICP atomic emission spectrometer INTEGRA XL (GBC,

Table 1 Definitions of grinding conditions

Grinding	Type of mill	Time of grinding/s	Frequency/Hz
G0	None	—	—
G1	Conventional vibration	10	60
G2	Conventional vibration	120	60
G3	Cryogenic	18	10
G4	Cryogenic	360	10

Dandenong Australia), equipped with a ceramic V-groove nebulizer (Glassexpansion, Australia) and a glass cyclonic spray chamber (Glassexpansion, Australia). The standardised methodology previously validated for measurement of geological samples was used. The value of validated uncertainty of the V concentration analysis was 0.049%.

To modify the sample particle size and dispersion, two techniques were chosen: grinding using conventional vibratory or cryogenic mills (see Table 1). In all cases of grinding, approximately 0.250 g of the sample was weighed.

Using the conventional ball vibration mill (model 3110-3A, Nicolet, USA), two sample sets were prepared. In the first case (G1), the powder was ground for 10 seconds and in the second case (G2), it was ground for 2 minutes, both with a frequency of 60 Hz. The cryogenic impact grinder with a self-contained liquid nitrogen bath (4–5 l) Model 6750 Freezer Mill (Spex, Certiprep, USA) operated at the liquid nitrogen temperature was used to prepare another set of samples. The pulverization of frozen samples was carried out by a magnetically shuttling steel impact bar back-and-forth against two stationary end plugs closing a cylindrical polycarbonate vial. Model 6751C20 grinding vials (volume 25 ml) were used for all performed experiments. Two operating programs (for sample sets G3 and G4) of the grinding equipment were utilized. One grinding step with a duration of 18 s was used for G3. Three grinding steps with a duration of 2 minutes and a resting period between particular steps with a duration of 2 minutes were used for G4. The pre-cooling time (a period before grinding, when a vial was immersed in liquid nitrogen for the purpose of sample freezing) was 2 minutes in both cases. The impact bar frequency (the number of back-and-forth movements of an impact bar per second) of 10 Hz was applied to all grinding programs.

The average particle sizes and the average particle size distributions have been verified by scanning electron microscopy (SEM). The granulometry of typical representative ground samples was realized by a SEM JEOL JSM-5500LV at an acceleration voltage between 10 and 20 kV. The grain analysis was performed using Gwyddion software (version 2.7) based on the derivation of a gray-scale signal for determination of grain boundary and, consecutively, a diameter of a circle with similar area. Powder samples (untreated and ground) were visualized by SEM sputtered on the slide and deposited on the surface of adhesive tape. First, one approach offers better spatial resolution and it was used for evaluation of grinding process quality (Fig. 1a and b); the second one with lower spatial resolution was used for the characterisation of samples subsequently analysed by LIBS (Fig. 2a–c).

Based on our previous experiences with such type of analytes, the deposition of powdered samples on the adhesive tape surfaces was adopted as a sample preparation method. For each sample, the homogeneous powder obtained from grinding was poured on the surface of adhesive tape with an area of 2 cm × 3 cm and spread by a soft brush. We assume that the sample applied on the tape creates a continuous close-to monolayer of particles. Such a thin layer is ideal for investigation and description of processes related to the influence of granulometry (and so the matrix effect) in the LIBS measurements.

LIBS instrumentation

The influence of the matrix effect on LIBS outcomes was investigated using three LIBS devices with significantly different parameters.

The commercially available compact LIBS setup (LEA S500, Solar TII Ltd., Belarus), in the following text named as LS1, has a dual pulse Q-switched Nd:YAG laser operating at 1064 nm. The laser emits two co-linear pulses of about 12 ns duration with variable energy per pulse, which can be set from 80 to 150 mJ at a maximum repetition rate of 20 Hz. The interpulse delay can be set from 0 to 20 ms. The Czerny Turner spectrograph, with a focal length of 500 mm and a grating of 1800 lines mm^{-1}, provides a linear reciprocal dispersion of 1 nm mm^{-1}. The spectrograph is fully sealed and can be purged by a low flow of argon, so the wavelength range of the spectrograph is from 170 to 800 nm. Recording of the spectra is carried out by means of

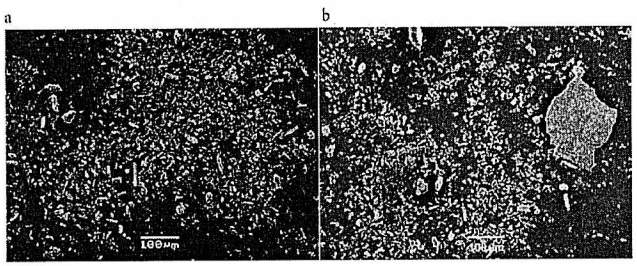

Fig. 1 SEM visualization of the mesoporous V–SiO_2 catalyst sample after short conventional grinding G1 (a) and long conventional grinding G2 (b) on the slide.

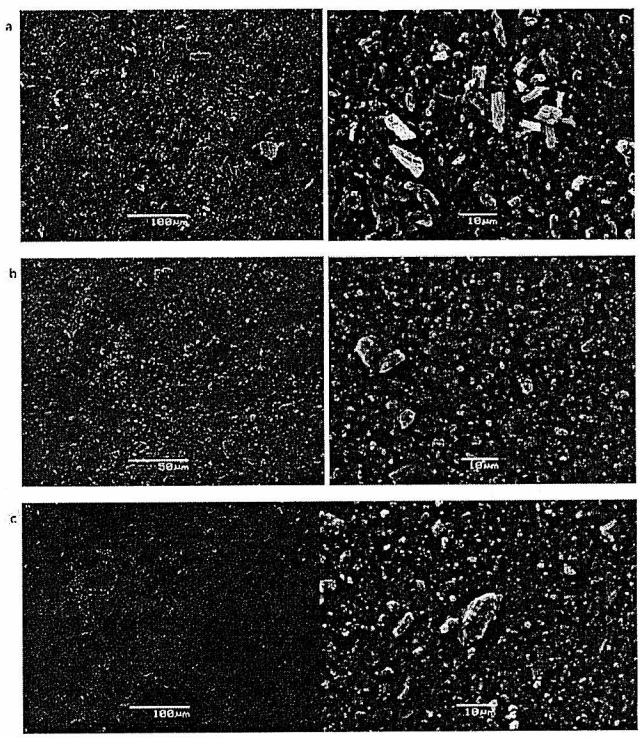

Fig. 2 SEM visualization of untreated sample of mesoporous V–SiO_2 catalyst (G0 grinding) (a) sample after G3 grinding (b) and after G2 grinding (c) on the tape.

a back thinned and front illuminated CCD-camera (2048 × 14 pixels) with a minimal integration time of 1 ms. Spectra can be measured in 30 nm wide regions. The samples are placed inside the sample chamber on the top of the motorized positioning table and the samples can be automatically moved during the analysis. Selection of the analyzed area on the sample surface is performed *via* an inbuilt video system with a magnification up to 100×. The measurements are fully software controlled (position and number of points in the pattern). In this study, the LIBS analysis was performed with a focal spot diameter of 200 μm, a laser pulse energy of 90 mJ, one laser shot per analytical point, 4 analytical points per sample and a spectrometer slit width of 15 μm.

The table-top laboratory LIBS setup, in the following text named as LS2, and in detail described elsewhere,[21] is used as a primary laser source pulsed Nd:YAG laser (Brilliant b, Quantel, France B), with a typical pulse repetition rate of 10 Hz. The pulse energy can be set up to 450 (900) mJ per pulse for wavelengths 532 (1064) nm, respectively. The beam diameter at the aperture was 8 mm. A vacuum interaction chamber (LM, Tescan s.r.o., Czech Republic), which includes a 3-axes manipulator, laser focusing optics, plasma emission collecting optics, illumination, gas inlet (Ar and He) and vacuum pumps, was used. A CCD camera for sample positioning is mounted on the top of the chamber. The detection system consists of a spectrometer (260i, Lot Oriel, USA) and a coupled ICCD camera (iStar, Andor, Ireland). The setup was gated by a pulse generator (DG-535, Stanford Research System, Inc., USA). The LIBS spectra were recorded with the following parameters: the focal spot diameter was 350 μm, laser pulse energy 120 mJ, one laser shot per analytical point, 9 analytical points per sample, and spectrometer slit width 50 μm. As a typical delay time and gate width values of 850 ns and 15 000 ns, respectively, were used.

The second table-top modular laboratory LIBS setup, in the following text named as LS3, and in detail described in Kaski *et al.*,[22] utilized an ArF excimer laser (Optex, Lambda Physik, USA) operated at a fundamental wavelength (193 nm) at a repetition rate of 5 Hz and a pulse width of 8 ns. The laser beam was focused at a 30° angle to the target surface *via* a fused silica lens with a focal length of 40 mm. The Czerny-Turner spectrograph (Acton Research, SP-150, USA) with focal length 150 mm and holographic UV grating (2400 grooves per mm, resolution ≈ 0.5 nm) and slit width ~10 μm was used. The spectra were recorded using an ICCD detector with a 1024 × 256 pixel imaging area and an 18 mm intensifier (InstaSpec V, Oriel, Germany). The detector was gated by a pulse generator (DG-535, Stanford Research System, Inc., USA). Typical delay time and gate width values of 100 ns and 1000 ns, respectively, were used. The laser spot diameters were 85 μm to 120 μm. The laser pulse energy was approximately 1.36 mJ.

Results and discussion

Sample characterization

The original particle size distribution of (vanadium-) silica ($V–SiO_2$) samples was modified using the selected grinding techniques.

The influence of grinding type and operating conditions of a particular mill on resulting granulometry was studied using SEM images. Fig. 1a and b were obtained by visualisation of the silica sample treated by conventional grinding with a duration of 10 s and 2 min, respectively. Visualised samples were sprinkled on the slide before SEM analysis. The formation of large-sized clusters during the long time conventional grinding is obvious. Fig. 2c shows SEM images of a long-time ground silica sample deposited on the surface of adhesive tape. As can be seen in this figure, the big clusters were not captured on the surface of adhesive tape. It can be concluded that using adhesive tape as a powder sample holder reduces the particle size of the analysed sample.

In the case of cryogenic grinding, the formation of large-sized clusters as a consequence of longer grinding time was not observed. Fig. 2 summarizes the results of the particle size analysis performed using SEM images of powder samples deposited on the adhesive tape surface. Table 2 summarizes the important statistical characteristics describing the particle size distribution.

On the basis of these results, it is clear that granulometry of $V–SiO_2$ catalyst samples is significantly affected by the preparation technique. Similar results were found for all concentrations of vanadium. Given the aforementioned characteristics of ground samples, for further experiments, sample sets G3, G2 and untreated samples (G0) were selected.

LIBS optimization

In general, the optimization of LIBS analysis is a complex task. It is necessary to find the best combination of at least seven basic parameters of LIBS equipment (energy of laser pulses, delay

Table 2 Diameter of circle with similar area (diameter), median of diameter (median), minimum and maximum of diameter (min–max), range of particle size distribution (range), kurtosis of particle size distribution (kurtosis), intensity of LIBS signal (intensity) and relative standard deviation (RSD %) of LIBS signal values for the sample under study

Particle size characterization						LIBS measurement	
Grinding	Diameter/μm	Median/μm	Min–max/μm	Range/μm	Kurtosis	Intensity[a]	RSD (%)[a]
G0	5.5	5.19	0.33–19.04	18.72	3.29	3.8×10^4	2.73
G1	3.1	2.34	0.54–15.70	15.16	6.51	4.1×10^4	4.54
G2	3.5	2.47	0.49–28.43	27.94	27.59	2.7×10^4	2.42
G3	1.7	1.45	0.24–7.07	6.83	2.37	5.0×10^4	0.88
G4	0.8	0.69	0.24–4.20	3.96	11.68	4.0×10^4	2.12

[a] Values from the LS1 device.

between pulses in the case of double-pulse LIBS, focal spot diameter, number of analytical points, spectrometer slit width, wavelength range of the spectrograph, number of pulses collected in one analytical point, *etc.*) providing satisfactory values of basic characteristics of the obtained analytical method (LOD, dynamical range, time consumption, *etc.*). The above-mentioned LIBS parameters are closely linked together and a minor change in one of them entails the necessity of a substantial change in the others. Development of the proper LIBS methodology is thus time consuming and large amounts of samples are consumed during this process.

Our optimization procedure is based on dividing LIBS parameters into fixed and variable ones. Fixed parameters are set in the beginning of the optimization process and they are not changed any more. Fixed parameters are set in the beginning of the optimization process with respect to the sample character and demands on the analytical process. The focal spot diameter and the number of analytical points are typical fixed parameters. In our case, we analyze precious samples with small surface, and minimization of the above-mentioned parameters is necessary for our ability to perform repeated measurements. The number of shots is another fixed parameter. The maximal value of this parameter is restricted by the thickness of used adhesive tape. The most important variable parameters are laser energy, inter-pulse delay and spectrometer slit width. These parameters strongly influence sensitivity and repeatability of measurements. They are optimized jointly and proper parameters are used for evaluation of measurement quality (SBR and RSD).

The optimization of LIBS parameters was performed on the sample with a mean concentration of vanadium—2.8 (w/w%) and with a narrow particle size distribution (G3). The 311.071 nm spectral line of vanadium, used in our previous work (Pouzar *et al.*[23]), was repeatedly measured (3 series—each with 4 shots), and then optimization criteria, signal/background ratio (SBR) and relative standard deviation (RSD%) values of the LIBS signal, were evaluated. Optimal parameters for each of the LIBS instruments used are listed in the corresponding part of the "Experimental" chapter.

Influence of granulometry on LIBS signal

The influence of the mean particle size and the particle size distribution on LIBS analysis was investigated on the LS1 device. Samples with the same concentration, as in the case of LIBS optimization, but with different particle size distributions were selected (Fig. 3). As can be seen from Table 2, at a given concentration, the intensity of the LIBS signal slightly correlates with the average particle size and median of the measured sample. The correlation coefficient calculated for signal intensity and mean particle size was $r = -0.42$ and for signal intensity and median of particle size was $r = -0.22$. Significantly higher correlations between the intensity of analytical line and the characteristics that describe the particle size distribution were detected. Specifically, the correlation between the LIBS signal intensity and the range of particle sizes was r 0.82 and between line intensity and kurtosis of particle size distribution was r 0.87. It can be concluded that samples with more uniform particle size distribution provide higher intensity of the LIBS analytical signal. Any similar significant correlation between statistical characteristics of particle size distribution and LIBS signal intensity was not observed.

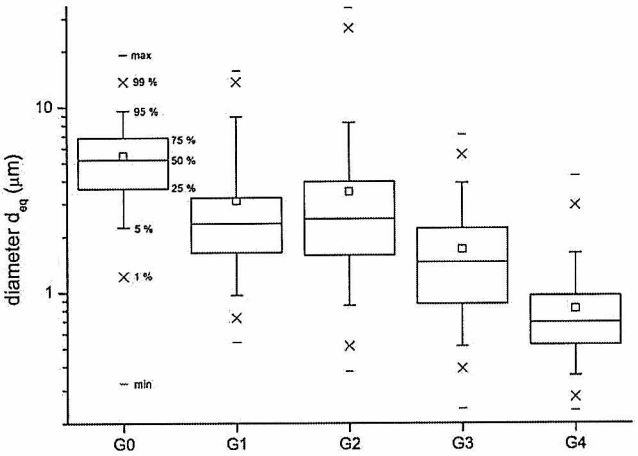

Fig. 3 Particle size distribution after different treatments for the sample under study.

Study of relationship between concentration of the element of interest in the sample and the signal intensity (*C–I* relationship)

Three groups of samples with different distributions of particles were selected for the study of the *C–I* relationship on each device. *C–I* curves were constructed under the above-mentioned optimised conditions and values of the regression characteristics and detection limits were obtained (Fig. 4–6). The concentration range of vanadium in the set of samples was 1.2–4.7 (w/w%). The first *C–I* curve (designated as G3) was measured for samples with a mean particle size of 1.7 µm and a 0.24–7.07 µm range of particle size distribution. The second *C–I* curve (designated as G2) was measured for samples with an average particle size of 3.5 µm and a 0.49–28.43 µm range of particle size distribution. The third *C–I* curve (designated as G0) was measured for samples with an average particle size of 5.5 µm and a 0.33–19.04 µm range of particle size distribution. Statistical characteristics of particular *C–I* curves are summarised in Table 3.

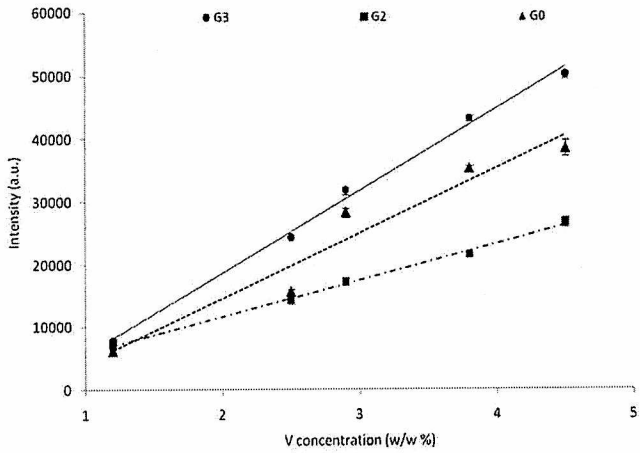

Fig. 4 *C–I* curves of V in catalyst for different grindings from the LS1 device.

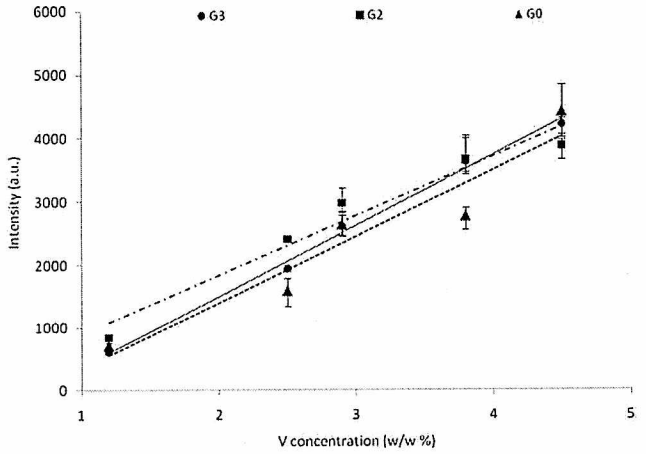

Fig. 5 *C–I* curves of V in catalyst for different grindings from the LS2 device.

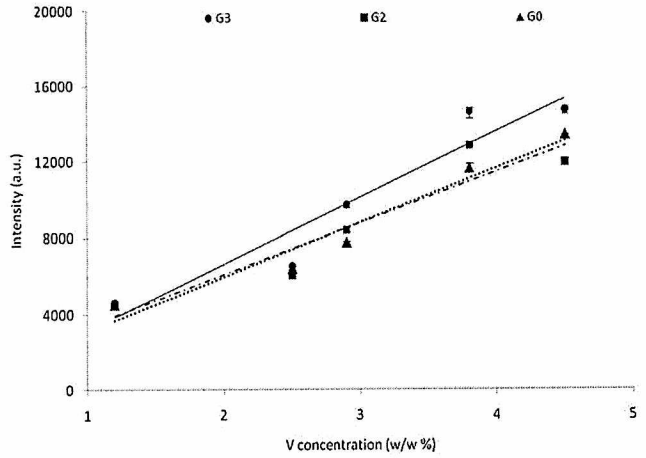

Fig. 6 *C–I* curves of V in catalyst for different grindings from the LS3 device.

For the LS1 device, the influence of sample particle size distribution on the *C–I* relationship is most noticeable. The above-mentioned relationship between the parameters describing the particle size distribution and intensity of the LIBS analytical signal was also reflected in the slope of the *C–I* curve. The smallest slope of the *C–I* curve was calculated for samples G2 (the widest particle size distribution) and conversely the highest slope was obtained for the G3 (the narrowest distribution). For the *C–I* curves, the statistical test of homogeneity of slopes was performed. The calculated value of the testing criterion F_S 16.3 was higher than its corresponding critical value $F_{0,95}$ (2, 9) 4.26 of this test; thus, the difference between slopes for the LS_1 *C–I* curves could be considered statistically significant. A similar influence of particle size distribution on the *C–I* curve slope was observed for LS_2 and LS_3 equipment as well. The maximal slope was obtained for G3 samples and minimal for G2 ones. However, these differences were not found to be statistically significant. The calculated values of the F_s criterion for the slope homogeneity test were 1.34 for the LS2 device and 0.6 for the LS3 device.

The best fitted *C–I* curve (minimal value of AIC, maximal value of R^2) for G2 samples was obtained in the case of the LS_1 setup, the LS_2 *C–I* curve was best fitted for G3 samples and the LS_3 *C–I* curve for G0 ones. Thus, no significant relationship between the particle size distribution characteristics and the level of *C–I* curve fit was observed.

The LOD was defined according to the $3\sigma/\beta$ concept, where σ was the standard deviation in the background calculated from three (3 series—each with 4 shots) replicated determinations of vanadium in the real sample with a low vanadium concentration (1.2 w/w%) and β was a slope of the *C–I* curve. For all LIBS setups, the lowest values of LODs were obtained when the *C–I* curves were constructed using G3 samples and the highest, when G0 samples were analyzed (Table 3). The values of LODs were better correlated with the mean particle size than with characteristics of particle size distribution. The best values of LODs were obtained for the LS1 setup, which offers the highest sensitivity (Fig. 4–6); second best ones were obtained for the LS3 device with best repeatability (error bars in Fig. 4–6). The worst LODs were obtained for the LS2 setup with the worst sensitivity and repeatability. The highest sensitivity of the LS1 device could be connected with using the double-pulse mode, while the devices LS2 and LS3 worked in single-pulse. The best repeatability of the LS3 device was probably connected using the excimer laser, which had better pulse to pulse energy stability than Nd:YAG lasers of LS1 and LS2 devices.

Influence of matrix characteristic

In our previous work (Pouzar *et al.*[23]), the differences in LIBS analysis outcomes of vanadium doped catalysts were interpreted as influences of the different vanadium chemical forms in samples. However, the sample grain size was not taken into

Table 3 Statistical characteristics of *C–I* curves: intercept of the curve (Intr), slope of the curve (β_1), Akaike information criterion (AIC), coefficient of determination (R^2) and limit of detection (LOD) of LIBS signal values for the sample under study

Device	Grinding	Intr	β_1	AIC	R^2	LOD (w/w%)
LS1	G3	-7.6×10^3	1.3×10^4	73	0.995	1.2×10^{-2}
	G2	-9.2×10^0	5.8×10^3	64	0.996	2.0×10^{-2}
	G0	-6.2×10^3	1.0×10^4	84	0.940	2.8×10^{-2}
LS2	G3	-7.5×10^2	1.1×10^3	49	0.995	3.9×10^{-2}
	G2	-4.0×10^1	9.4×10^2	58	0.954	6.3×10^{-2}
	G0	-7.1×10^2	1.0×10^3	63	0.917	1.3×10^{-1}
LS3	G3	-3.0×10^2	3.5×10^3	75	0.912	3.3×10^{-2}
	G2	-7.3×10^2	2.7×10^3	74	0.876	4.0×10^{-2}
	G0	-2.7×10^2	2.8×10^3	70	0.951	6.2×10^{-2}

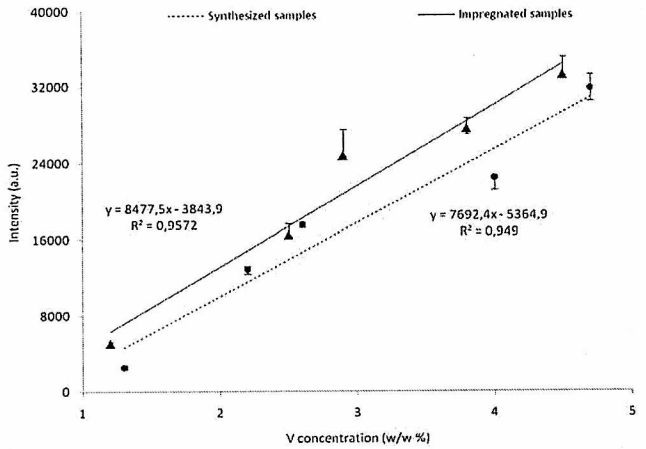

Fig. 7 *C–I* curves of V in catalyst for impregnated samples (triangles) and synthesized samples (squares) with similar granulometry from the LS1 device.

account. Therefore, to compare the influence of grain size and the influence of the vanadium chemical forms in the sample, samples with similar concentrations of vanadium and with the similar granulometry and size of particles, but with a different structure of the sample (synthesized and impregnated samples), were selected. It was thus possible to observe only the influence of the different sample structure without the influence of granulometry. In order to obtain samples with similar particle size and granulometry, it was necessary to use different types of grinding. For impregnated samples, which had a fibrous structure grinding procedure as described for G4, sample set preparation was used (the fiber length was changed) and for synthesized samples, the grinding procedure for G1 sample set preparation was used (the particle diameter was changed). After these adjustments, the ratio of diameter/particle distribution for both samples was the same. The particle size distributions of the ground impregnated samples were 0.4–1.6 μm and of the ground synthesized samples 0.2–1.2 μm.

As can be seen from Fig. 6, the influence of the sample structure was not significant. The Chow test proved that the difference of slopes and variances of corresponding *C–I* curves was not statistically significant. The calculated value of the testing criterion F_C 2.63 was lower than the corresponding critical value $F_{0.95}$ (2, 6) 5.143. *C–I* curves are very similar, and only for higher concentrations is it possible to observe differences between synthesized and impregnated samples (Fig. 7). It is necessary to emphasize that granulometry and the particle size of synthesized and impregnated samples were not totally identical. This probably caused the difference between the *C–I* curves for impregnated and synthesized samples, rather than the effect of the sample structure. However, the granulometry effect seems to be much stronger than the structural effect.

Conclusion

In this paper, the effect of particle size and granulometry in LIBS quantitative analysis of vanadium in hexagonal mesoporous silica catalysts has been discussed. The LIBS analysis was realized using three different LIBS devices. By two techniques of grinding, samples with a various granulometry were prepared. Deposition of the powdered samples on the surface of adhesive tape was adopted as a sample preparation method. A series of samples with different particle sizes were used to construct the *C–I* curves. The obtained results indicated that sensitivity of LIBS measurements was seriously affected by particle size distribution of the sample. This effect was the most obvious for devices offering the analytical signal with highest sensitivity and sufficient repeatability. However, LOD values reflecting both sensitivity and repeatability of measurements were strongly influenced by the mean particle size.

Furthermore, we concluded that the influence of vanadium chemical forms in samples was insignificant for LIBS analysis. If samples for LIBS analysis are prepared by grinding, it is best to use short cryogenic grinding to ensure the samples with narrow particle size distribution and minimize the clusters. It is also very important to unify the conditions of grinding to obtain samples with the same granulometry and thus the effect of particle size distribution in LIBS analysis can be minimized. Ideally, a standard and a sample should have the same granulometry.

Acknowledgements

The authors gratefully acknowledge the financial support from the project MSM 0021627501 and MSM 0021627502. J.K. acknowledges the support from the Ministry of Education, Czech Republic on the frame of project ME10061.

References

1 *Laser Induced Breakdown Spectroscopy*, ed. A. W. Miziolek, V. Palleschi and I. Schechter, Cambridge University Press, Cambridge, 2006.
2 D. A. Cremers and L. J. Radziemski, *Handbook of Laser-Induced Breakdown Spectroscopy*, John Wiley and Sons Ltd., Chichester, 2006.
3 *Laser-Induced Breakdown Spectroscopy*, ed. J. P. Singh and S. N. Thakur, Elsevier, Amsterdam, 2007.
4 M. Hola, V. Konecna, P. Mikuska, J. Kaiser, K. Palenikova, S. Prusa, R. Hanzlikova and V. Kanicky, *J. Anal. At. Spectrom.*, 2008, **23**(10), 1341–1349.
5 M. Hola, V. Konecna, P. Mikuska, J. Kaiser and V. Kanicky, *Spectrochim. Acta, Part B*, 2010, **65**, 51–60.
6 R. Barbini, F. Colao, R. Fantoni, V. Lazic, A. Palucci, F. Capitelli and H. J. L. van der Steen, *EARSeL eProceedings*, 2001, **1**, 122–129.
7 C. Chaléard, P. Mauchien, N. Andre, J. Uebbing, J. L. Lacour and C. Geertsen, *J. Anal. At. Spectrom.*, 1997, **12**, 183.
8 U. Panne, C. Haisch, M. Clara and R. Niessner, *Spectrochim. Acta, Part B*, 1998, **53**, 1957.
9 J. B. Ko, W. Sdorra and K. Niemax, *Fresenius' Z. Anal. Chem.*, 1989, **335**, 648.
10 R. Barbini, F. Colao, R. Fantoni, A. Palucci, S. Ribezzo, H. J. L. van der Steen and M. Angelone, *Appl. Phys. B: Lasers Opt.*, 1997, **65**, 101–107.
11 W. Tawfik, *Progr. Phys.*, 2007, **2**, 42–49.
12 O. V. Borisov, X. L. Mao, A. Fernandez, M. Caetano and R. E. Russo, *Spectrochim. Acta, Part B*, 1999, **54**, 1351.
13 V. Margetic, K. Niemax and R. Hergenroder, *Spectrochim. Acta, Part B*, 2001, **56**, 1003.
14 V. Bulatov, R. Krasniker and I. Schechter, *Anal. Chem.*, 1998, **70**, 5302.
15 R. Krasniker, V. Bulatov and I. Schechter, *Spectrochim. Acta, Part B*, 2001, **56**, 609.
16 A. K. Kningt, N. L. Scherbarth, D. A. Cremers and M. J. Ferris, *Appl. Spectrosc.*, 2000, **54**, 331.
17 A. S. Eppler, D. A. Cremers, D. D. Hickmott, M. J. Ferris and A. C. Koskelo, *Appl. Spectrosc.*, 1996, **50**, 1175.
18 M. A. Ismail, H. Imam, A. Elhassan, W. T. Youniss and M. A. Harith, *J. Anal. At. Spectrom.*, 2004, **19**, 489–494.

19 S. I. Gornushkin, I. B. Gornushkin, J. M. Anzano, B. W. Smith and J. D. Winefordner, *Appl. Spectrosc.*, 2002, **56**, 433–436.
20 J. M. Anzano, M. A. Villoria, A. Ruíz-Medina and R. J. Lasheras, *Anal. Chim. Acta*, 2006, **575**, 230–235.
21 J. Kaiser, M. Galiova, K. Novotny, R. Cervenka, L. Reale, J. Novotny, M. Liska, O. Samek, V. Kanicky, A. Hrdlicka, K. Stejskal, V. Adam and R. Kizek, *Spectrochim. Acta, Part B*, 2009, **64**, 67–73.
22 S. Kaski, H. Hakkanen and J. Korppi-Tommola, *Miner. Eng.*, 2003, **16**, 1239–1243.
23 M. Pouzar, T. Kratochvíl, L. Čapek, L. Smoláková, T. Černohorský and A. Krejčová, *Talanta*, 2011, **83**, 1659–1664.